

1 **Computational vaccinology based development of multi-epitope** 2 **subunit vaccine for protection against the Norovirus' infections**

3 Irfan Ahmad^{1#}, Syed Shujait Ali^{1#}, Ismail Shah¹, Shahzeb Khan¹, Mazhar Khan⁵, Saif Ullah¹,
4 Shahid Ali¹, Jafar Khan¹, Mohammad Ali¹, Abbas Khan^{2*}, Dong-Qing Wei^{2*}

5 ¹Centre for Biotechnology and Microbiology, University of Swat, Swat, Khyber Pakhtunkhwa,
6 Pakistan.

7 ²Department of Bioinformatics and Biological statistics, School of Life Sciences and
8 Biotechnology, Shanghai Jiao Tong University, Shanghai 200240, P.R China.

9 ³State Key Laboratory of Microbial Metabolism, Shanghai-Islamabad-Belgrade Joint Innovation
10 Center on Antibacterial Resistances, Joint Laboratory of International Cooperation in Metabolic
11 and Developmental Sciences, Ministry of Education and School of Life Sciences and
12 Biotechnology, Shanghai Jiao Tong University, Shanghai 200030, P.R. China

13 ⁴Peng Cheng Laboratory, Vanke Cloud City Phase I Building 8, Xili Street, Nashan District,
14 Shenzhen, Guangdong, 518055, P.R China.

15 ⁵The CAS Key Laboratory of Innate Immunity and Chronic Diseases, Hefei National Laboratory
16 for Physical Sciences at Microscale, School of Life Sciences, CAS Center for Excellence in
17 Molecular Cell Science, University of Science and Technology of China (USTC), Collaborative
18 Innovation Center of Genetics and Development, Hefei, 230027, Anhui, China.

19 Irfan Ahmad

20 irfanmicrouos@gmail.com

21 Syed Shujait Ali, PhD

22 shujaitswati@uswat.edu.pk

23 Shahzeb Khan

24 khanshahxeb173@gmail.com

25 Mazhar Khan

26 mazharsw@mail.ustc.edu.cn

27 Abbas Khan(corresponding author)

28 abbaskhan@sjtu.edu.cn

29 Saif Ullah

30 Usaif7454@gmail.com

31 [Shahid Ali](#), PhD

32 shahidali@uswat.edu.pk

33 [Jafar Khan](#), PhD

34 Jafar@uswat.edu.pk

35 [Mohammad Ali](#), PhD

36 alimoh@uswat.edu.pk

37 Dong-Qing Wei, PhD (corresponding author)

38 dqwei@sjtu.edu.cn

39 **# CONTRIBUTED EQUALLY**

40

41

42

43 **Abstract**

44 Human Norovirus belong to family *Calciviridae*, it was identified in the outbreak of
45 gastroenteritis in Norwalk, due to its seasonal prevalence known as “winter vomiting disease”.
46 Treatment of Norovirus infection is still mysterious because there is no effective antiviral drugs
47 or vaccine developed to protect against the infection, to eradicate the infection an effective
48 vaccine should be developed. In this study capsid protein (A7YK10), small protein (A7YK11)
49 and polyprotein (A7YK09) were utilized. These proteins were subjected to B and T cell epitopes
50 prediction by using reliable immunoinformatics tools. The antigenic and non-allergenic epitopes
51 were selected for subunit vaccine, which can activate cellular and humoral immune responses.
52 Linkers joined these epitopes together. The vaccine structure was modelled and validated by
53 using Errat, ProSA and rampage servers. The modelled vaccine was docked with TLR-7.
54 Stability of the docked complex was evaluated by MD simulation. In order to apply the concept
55 in a wet lab, the reverse translated vaccine sequence was cloned in pET28a (+). The vaccine
56 developed in this study requires experimental validation to ensure its effectiveness against the
57 disease.

58

59

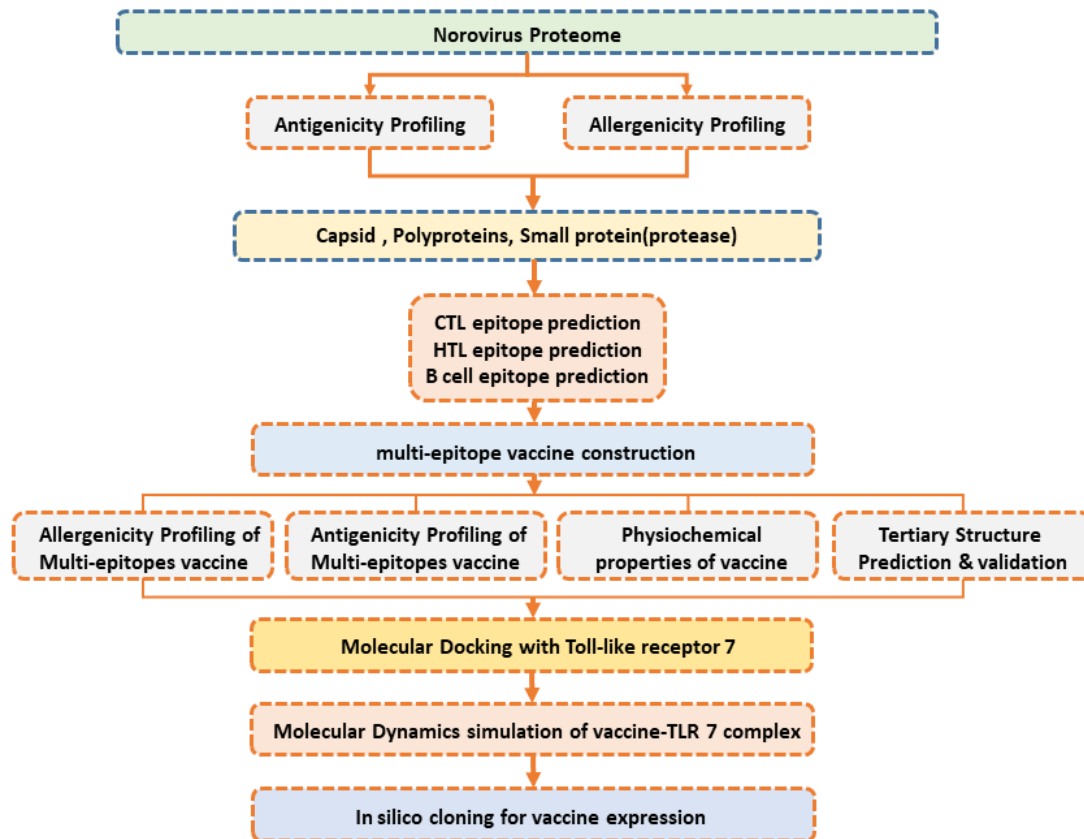
60 **Introduction**

61 Norovirus (NVs), also known as “small round-structured virus” and this RNA single-stranded
62 virus is placed within family *Caliciviridae*. NVs is responsible for the spread of non-bacterial
63 human gastroenteritis (1). The Human norovirus (HuNV) was first identified in stool specimen,
64 during gastroenteritis outbreak in Norwalk and was coined as Norwalk virus. More than a
65 thousand strains of NVs are isolated which are genetically and serologically different. The
66 infected person has an abdominal cramp, stomach pain, diarrhoea, vomiting and nausea with
67 mild pyrexia (2). The consumption of contaminated food and water is deemed essential for the
68 development and spread of disease (3), (4), and globally 20 % of all diarrheal diseases are caused
69 by HuNV, and nearly 21200 victims succumbed to death annually (5, 6). HuNV interferes with
70 interferon type I & III by influencing MHC-I expression and causing rapid infection. MHC-I
71 plays a key role in providing immunity against viruses. In this process, proteasome-mediated
72 degraded peptides are presented to the CD8+ T-cells for evoking immune reactions (7). The
73 genome of HuNV is 7.5 kb, which consists of three open reading frames (ORF's), ORF1, ORF2,
74 and ORF3. These ORF's (ORF1, ORF2, and ORF3) codes for a nonstructural protein, VP1 major
75 capsid protein, and VP2 minor capsid proteins respectively (8).

76 In clinical samples, an electron microscope (EM) (9) is used as a diagnostic tool for norovirus
77 identification. ELISA (enzyme-linked immunosorbent assay) and molecular techniques are
78 accessible for the diagnostic purpose of pathogens including norovirus. EM is found in the well-
79 equipped lab and it is used to look for the pathogenic particles in the feces. RT-PCR (10) shows
80 sensitivity for identification, and it also assist in comprehension of these viruses molecular
81 diversity (11-15). Genomic characterization and molecular diversity is assessed by (HMA)
82 hetero duplex mobility assay of various viruses which include; Norovirus (16), measles virus
83 (17), polioviruses (18), hepatitis C virus (19) and polioviruses (18). Cross challenge studies and
84 IEM (immune electron microscopy) studies (20) was previously utilize for NV antigenic
85 diversity assessment, before the development of rNV (recombinant-NV) capsid protein.

86 Non-bacterial gastroenteritis is still a great challenge, and there is no effective licensed vaccine
87 available for its treatment (7). Researchers are trying their best to launch an effective vaccine
88 against norovirus, however, their investigations are either in clinical trials or in pre-clinical
89 stages (21). These investigations may results in two norovirus vaccines in future, bivalent
90 GI.1/GII.4 intramuscular VLP vaccines (in phase II b clinical trial), and monovalent GI.1 oral
91 pill recombinant adenovirus vaccine (phase I trials) (7). NoV infection is equally pervasive in
92 developing as well as developed countries. Children and elders are severely affected by these
93 infections. Effective vaccines and drug designing would be instrumental in controlling the higher
94 mortality rates caused by these infections (6). Vaccines evoke innate and cellular immune
95 responses to develop antibodies and memory cells, which may provide long-lasting protection
96 from specific serotypes (22). In-silico study based on immunoinformatics approaches was
97 applied to pinpoint effective epitopes or hits as a potential candidate for vaccine or drug
98 designing (23-27). Computational approaches are beneficial to predict the antigen without
99 culturing the pathogenic strain experimentally (28-32).

100 In this study, computational analysis was performed to predict the epitopes based effective
101 vaccine against the NoV. T-cell, B-cell and HTL epitopes were predicted and analyzed using
102 defined criteria for selecting the potential epitopes for final vaccine construct. Further
103 implementation of molecular docking with TLR receptors, molecular dynamics simulation and
104 codon optimization for expression confirmed the potential of the final vaccine construct. Thus,
105 this study provides a way towards the development of a potential vaccine candidate against the
106 Norovirus.



124 **Figure. 1.** Schematic representation of the steps involved in epitope-based vaccine designing. A
125 multi-step approach was used to construct the final vaccine candidate. Finally, validation through
126 MD simulation and in silico expression was achieved.

128 Results

129 Protein collection

130 The amino acid sequences of capsid protein (UniProt id: A7YK10), polyprotein (UniProt id:
131 A7YK09) and small protein (A7YK11) of *Norovirus* as well as Beta-defensin 3 (Q5U7J2), an
132 adjuvant was retrieved from UniProtKB in FASTA format. These protein were antigenic in
133 nature based on antigenicity score of 0.48, 0.52, and 0.49 respectively as calculated by VaxiJen
134 server and were selected for the designing of a multi-epitope vaccine by immunoinformatics
135 approach.

136

137 **CTL (Cytotoxic T Lymphocytes) epitopes prediction**

138 NetCTL1.2 server predicted a total of 51 CTL epitopes of 9-mer in length. In these epitopes, six
 139 non-allergenic epitopes (**Table 1**) were selected for vaccine designing based on high binding
 140 affinity score. Based on the predicted scores, two epitopes were selected from A7YK09,
 141 A7YK10 and A7YK11 each.

142

143 **Table 1.** Selected CTL epitopes. All the epitopes are based on their scores.

Proteins	Sequence ID	Peptide	Affinity	affinity rescale	Cleavage	TAP	Combine score	MHC binding Epitope
A7YK10	469	QSDALLIRY	0.7635	3.2418	0.9510	2.8490	3.5269	Yes
	91	YLAHLSAMY	0.5251	2.2294	0.8881	2.7960	2.5024	Yes
A7YK09	1044	TSSGDFLKY	0.5906	2.5076	0.9717	2.9870	2.8027	Yes
	1513	MQESEFSFY	0.5161	2.1913	0.5334	2.9500	2.4188	Yes
A7YK11	122	AVDWSGTRY	0.5730	2.4330	0.9756	3.1630	2.7375	Yes
	140	FSGGFTPSY	0.3257	1.3828	0.9690	2.6770	1.6620	Yes

144

145 **HTL (Helper T lymphocytes) prediction**

146 MHC-II prediction module of IEDB was used for Helper T Lymphocytes (HTL) epitopes
 147 prediction for HLA-DRB1*01:01, HLA-DRB1*01:02, HLA-DRB1*01:03, HLA-DRB1*01:04,
 148 and HLA-DRB1*01:05 Human alleles.. 9 HTL epitopes with the highest binding affinity were
 149 selected. The selected epitopes are situated at position 145-159,373-387,117-131 (capsid
 150 protein), 1-15, 1631-1645, 816-830, 617-631, 1089-1103 and 193-207 (polyproteins). (Table 2
 151 represent selected HTL epitopes).

152

153 **Table 2:** HTL selected epitopes. The epitopes are based on percentile rank.

Proteins	Allele	Start	End	Peptide	Method	Percentile rank
Capsid protein	HLA-DRB1*01:02	145	159	PHVMCDVRALEPIQL	sturniolo	0.02
	HLA-DRB1*01:03	373	387	KVYASLAAAAPLDLV	NetMHCIIpan	0.20
	HLA-DRB1*01:02	117	131	FTAGKVVVALVPPYF	sturniolo	0.44
Polyprotein	HLA-DRB1*01:02	1	15	MRMATPSSASSVRNT	sturniolo	0.12
	HLA-DRB1*01:01	1631	1645	GEKYYRTVASRVSKE	Consensus (comb.lib./smm/nn)	0.19
	HLA-DRB1*01:03	816	830	ITSILQAAGTAFSIY	NetMHCIIpan	0.25
	HLA-DRB1*01:02	617	631	CRRIDFLVYAESPVV	sturniolo	0.32
	HLA-DRB1*01:03	1089	1103	LALAVRMGSQAAIKI	NetMHCIIpan	0.51
	HLA-DRB1*01:02	193	207	PLDPAELRKCVGMTV	sturniolo	0.59

154

155

156 **Interferon production**

157 Online server IFN-epitope was used to identify the HTL epitope with a potential to induce the
 158 release of IFN-gamma from T (CD4+) cell. This analysis resulted in three epitopes (out of nine
 159 HTL epitopes) with the ability to induce T cells for interferon production (**Table 3**).

160

161 **Table 3.** Selected HTL epitopes analysis for interferon production.

Serial No	Sequence	Method	Result	Score
1	PHVMCDVRALEPIQL	MERCI	NEGATIVE	1
2	GEKYYRTVASRVSKE	MERCI	NEGATIVE	1
3	ITSILQAAGTAFSIY	MERCI	NEGATIVE	1
4	CRRIDFLVYAESPVV	MERCI	NEGATIVE	1
5	KVYASLAAAAPLDLV	SVM	POSITIVE	0.32853096
6	FTAGKVVVALVPPYF	SVM	NEGATIVE	-0.37555421
7	MRMATPSSASSVRNT	SVM	POSITIVE	0.98957435
8	LALAVRMGSQAAIKI	SVM	POSITIVE	0.087092709
9	PLDPAELRKCVGMTV	SVM	NEGATIVE	-0.024602308

162

163 **B-cell epitope prediction for norovirus**

164 B-cell epitope prediction was performed on ABCpreds server and six epitopes of 20-mer in
 165 length with a score higher than 0.83 were selected for further analysis (**Figure 3A**).
 166 Conformational B-cell epitopes were identified on Discotope 2.0 and out of 359 residues, 50 B-
 167 cell residues were predicted. The predicted B-cell Linear and discontinuous epitopes are given in
 168 **Table 4** and **5**.

169 **Table 4:** Predicted Linear B cell epitopes with their respective scores.

Rank	Sequence	Score	Start position
1	GPGGEKYYRTVASRVSKEGP	0.91	222
2	VMCDVRALEPIQLGPGPGHV	0.89	127
3	GNSISTGPGPGGGGLMGIIG	0.87	334
4	LEPIQLPLLDGPGGMRMAT	0.86	190
5	PGPGPGVMCDVRALEPIQLP	0.86	159
6	PGPGITSILQAAGTAFSIYG	0.84	241

170

171 **Table 5.** Predicted discontinuous B-cell epitopes residues with their contact number and
 172 Discotope score.

S.NO	Residues	Contact number	Discotope score
1	LYS, TYR, PRO, GLN, ASN, GLY, PRO, GLY, GLY, GLU	3, 6, 4, 0, 4, 1, 0, 12, 2, 4	-2.885, -2.029, -3.589 -3.886, -1.879, 1.667 2.652, 3.693, 2.327, 0.024
2	LYS, PRO, TYR, GLY, PRO, GLY, PRO, GLY, HIS, GLY	8, 9, 11,13, 3, 13, 5, 0, 0, 6	-0.356, -2.670, -2.082, 1.008, 2.997, 4.536, 5.611, 5.290, 5.382, 5.370

3	GLU, LYS, TYR, TYR, ARG, THR, ALA, LYS, PRO, GLY	13, 9, 18, 32, 6, 3, 7, 0, 8, 4	5.690, 5.180, 4.948, 2.551, 1.623, 0.693, -2.447, -3.572, -2.696, -2.886
4	GLY, ILE, ILE, GLY, ASN, SER, ILE, GLY, PRO, GLY	4, 35, 7, 30, 3, 16, 3, 4, 13, 36	-1.302, 0.705, 2.215, 3.458, 5.151, 4.587, 2.787, 2.029, 0.101, 0.667
5	PRO, GLY, PRO, GLY, PRO, GLY, ILE, ASN, GLY, GLY	11, 28, 7, 0, 7, 12, 6, 0, 16, 15	-0.292, 0.722, 1.126, 1.693, 1.776, 1.315, -0.535, -2.624, 0.504, -2.062

173

174 Final multi-epitope vaccine construct

175 The final multi-epitope vaccine construct was composed of 6 CTL and 9 HTL epitopes selected
 176 based on high binding affinity scores. AAY linkers were used to combine CTL epitopes and
 177 GPGPG linkers joined HTL epitopes, Whereas EAAAK linker was used for attachment of
 178 adjuvant to the N-terminal of vaccine, which amplifies its function.

179

180 CTL epitopes

181

182

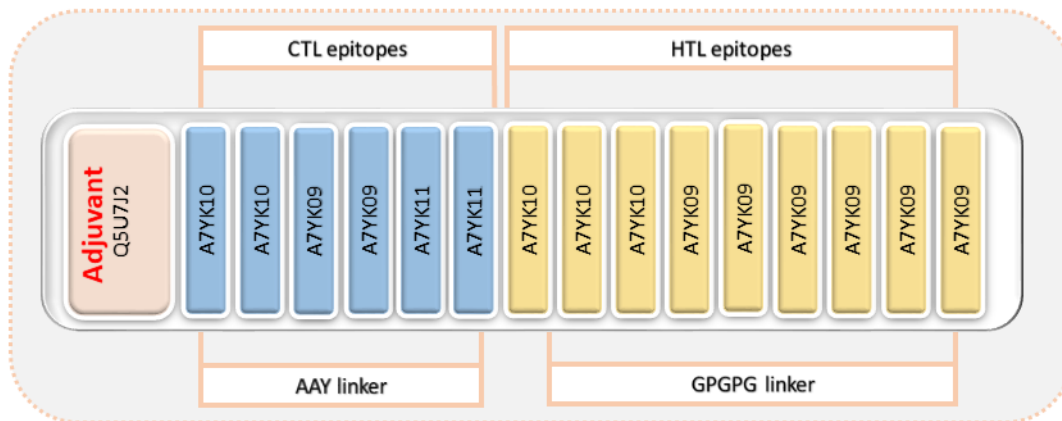
183

184

185

186

187



188 **Figure. 2.** Final vaccine construct. Six different CTL epitopes while nine HTL epitopes from
 189 three different proteins were combined to construct the multi-epitope subunit vaccine using
 190 linkers. An adjuvant to the N-terminal has also been added.

191

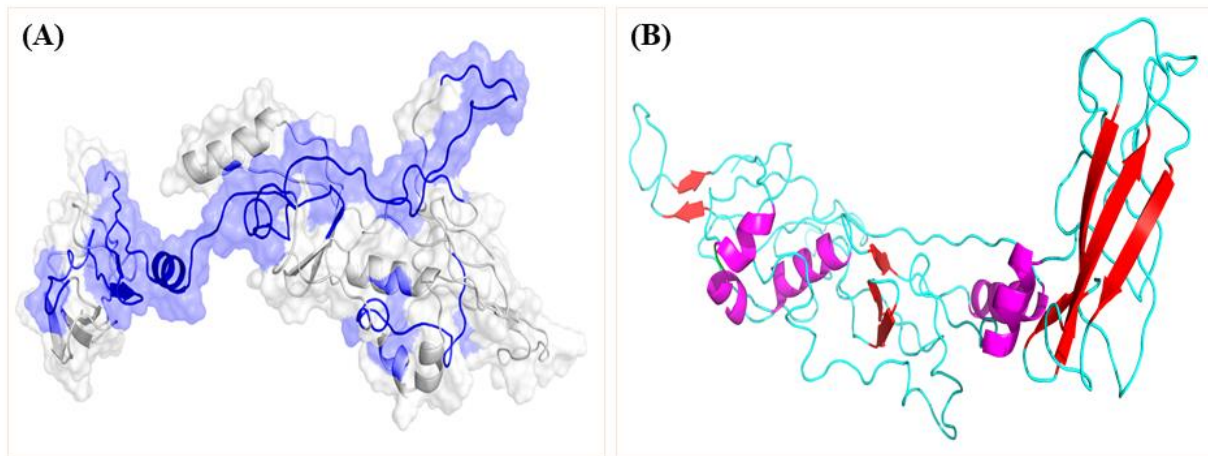
192 Prediction and validation of tertiary structure

193 3D structure of the vaccine was predicted on Robetta server. Five models were generated, and
 194 after evaluation model three (**Figure 3B**) was selected for further analysis. The selected model
 195 was validated by RAMPAGE, ProSA-web, and ERRAT (**Figure 4**). Modeled protein
 196 Ramachandran plot analysis revealed that most favored regions, additionally allowed regions,
 197 generously allowed region and disallowed region contain 81.1%, 6.8%, 1.2% and 0.4% of
 198 residues, respectively. ProSA-web and ERRAT were used for the evaluation of potential and
 199 quality errors in 3D crude model. Modeled protein overall quality factor was found 69.2%
 200 utilizing ERRAT. ProSA-web is utilized for prediction of Z-score prediction, which is found as -
 201 4.7.

202

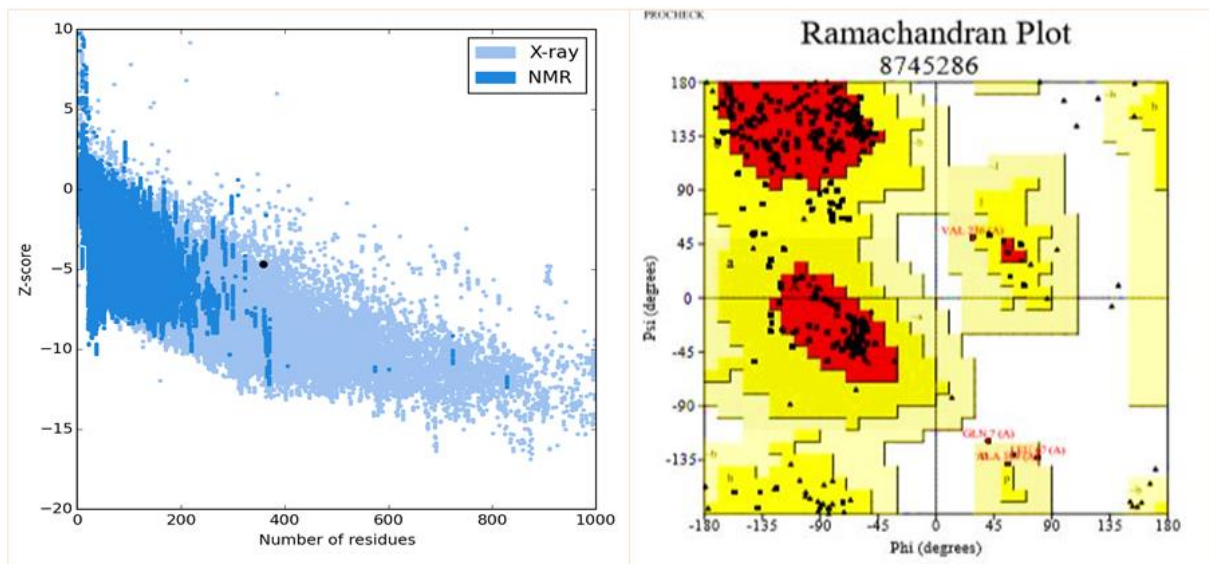
203

204
205
206
207
208
209
210
211
212
213
214
215
216



217 **Figure 3:** Predicted structure of the vaccine. (A) Showing the B-cell epitope (blue) (B) Showing
218 the final structure of multi-epitopes vaccine construct showing loops (cyan), Helix (magenta) and
219 beta-sheets (red).

220
221
222
223
224
225
226
227
228



229 **Figure 4:** Validation of 3D final vaccine model. (A) PROSA showing Z-score (-4.7) for 3D
230 structure validation (B) In Ramachandran analysis residues were allocated; most favoured region
231 81.1%, allowed 6.8%, generously allowed 1.2% and disallowed region 0.4% residues.
232

233 **Antigenicity, allergenicity and physiochemical parameter prediction of final vaccine**
 234 **construct**

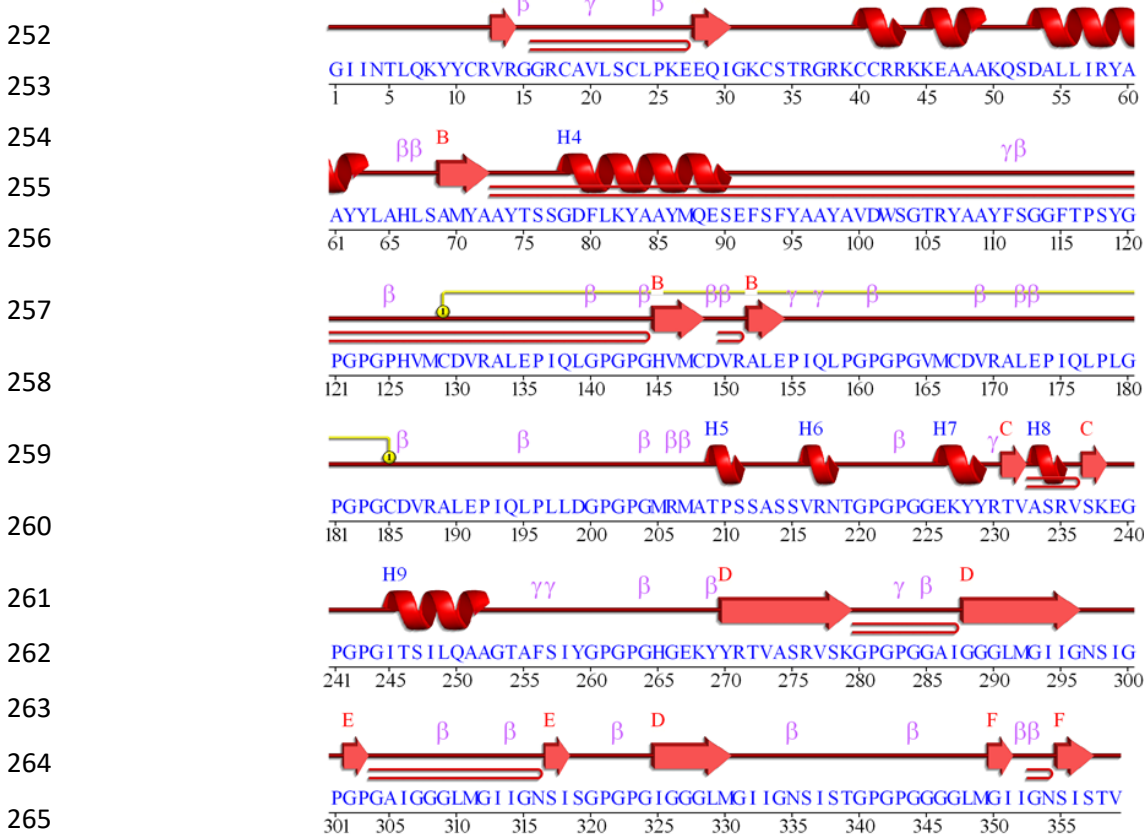
235 The antigenicity of the final vaccine construct was predicted on VaxiJen and ANTIGENpro
 236 servers by selecting bacteria model at 0.4% threshold. The antigenicity scores predicted by
 237 VaxiJen and ANTIGENpro are 0.8134% and 0.635949%, respectively, which indicates the
 238 antigenic nature of the final vaccine. For allergenicity, AlgPred was used and -0.62811 score
 239 indicating the non-allergen nature of vaccine using the default threshold of -0.40. The
 240 physiochemical parameters including molecular weight (MW) and theoretical isoelectric point
 241 value (PI) of vaccine were found 36.56 kDa and 9.17, respectively, as predicted by ProtParam.
 242 The PI value (9.17) suggesting the basic nature of the vaccine. Moreover, the half-life in
 243 mammalian reticulocytes, yeast, and *E. Coli* was found 30 hours (in vitro); 20 hours (in vivo),
 244 and 10 hours (in vivo), respectively. The instability index score of 34.03 refers to the stable
 245 nature of the protein. The GRAVY (Grand average of hydropathicity) and the aliphatic index
 246 was found 75.88 and -0.040, respectively.

247

248 **Prediction of secondary structure**

249 Secondary structure for vaccine predicted by PSIPRED program suggests the presence of
 250 20.89% alpha-helix, 16.71% beta-strand, and 62.39 % coil as shown in **Figure 5**.

251



266 **Figure 5:** Represent the secondary structure of the final vaccine construct in which alpha helix,
 267 beta-strands and coils were identified (20.89%, 16.71% and 62.39%).

268 Subunit vaccine molecular docking with an immune receptor (TLR-7)

269 For docking of TLR-7 was docked with the multi-epitopes vaccine, using an online server
270 ZDOCK. Overall, ten complexes were generated and the most suitable vaccine-TLR complex
271 was selected based on correct conformation and binding (**Figure 6**). The PDBsum server reported 90
272 interface residues with one salt bridge and eight hydrogen bonds were reported between the vaccine and
273 TLR-7.

274

275

276

277

278

279

280

281

282

283

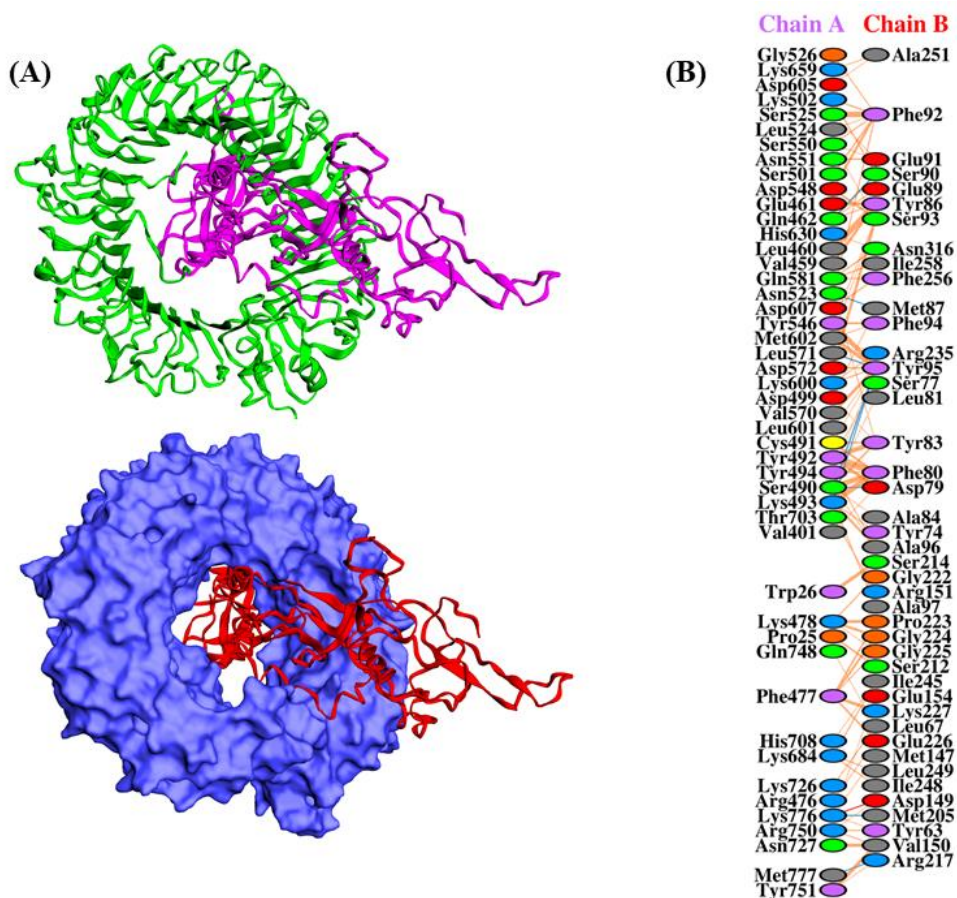
284

285

286

287

288



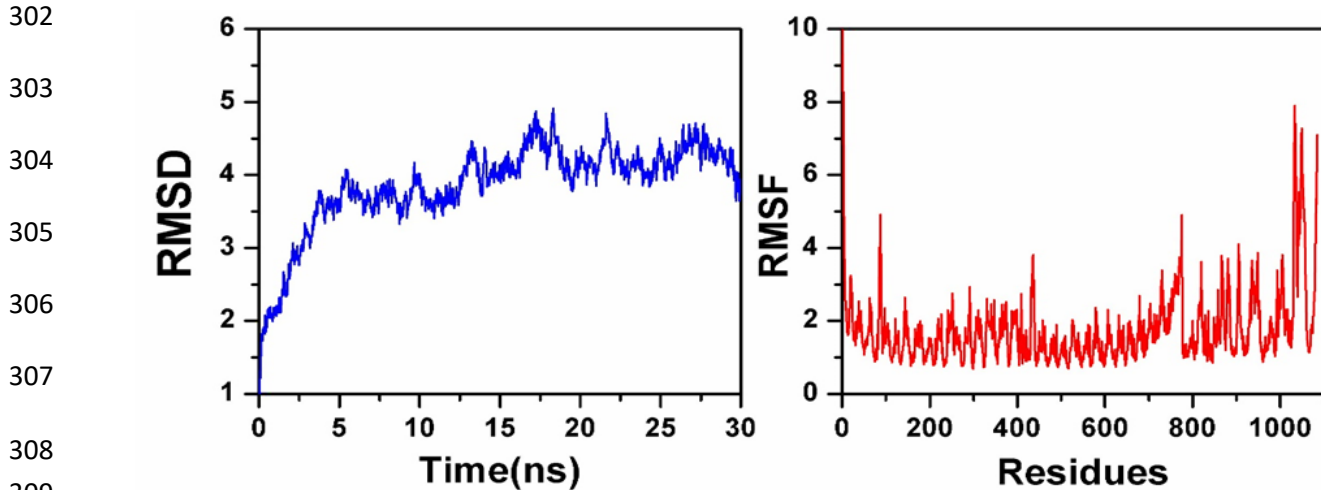
289 **Figure 6:** (A) TLR-7 (PDB ID: 5GMF) and vaccine docked complex. Magenta colour represents the
290 vaccine while the green and blue (surface) colour represents receptor. (B) Showing the interaction pattern
291 of the TLR-7 and vaccine construct.

292

293 MD simulation of immune receptor-vaccine complex

294 Molecular dynamics (MD) simulation was performed to check the stability and fluctuation of
295 vaccine construct and TLR-7 complex. The computed RMSD and RMSF for the vaccine
296 (protein) and its side chain as well as their graph are shown in **Figure 7**. The RMSD and RMSF
297 of protein and side-chain residues respectively were checked at 30ns time to estimate the stability
298 of the system. Overall fluctuation (RMSD) rate for the simulated system was found 4Å (TLR-7)
299 and RMSF (residual fluctuation) for maximum residues were found in acceptable range while
300 some residues exhibit higher fluctuation.

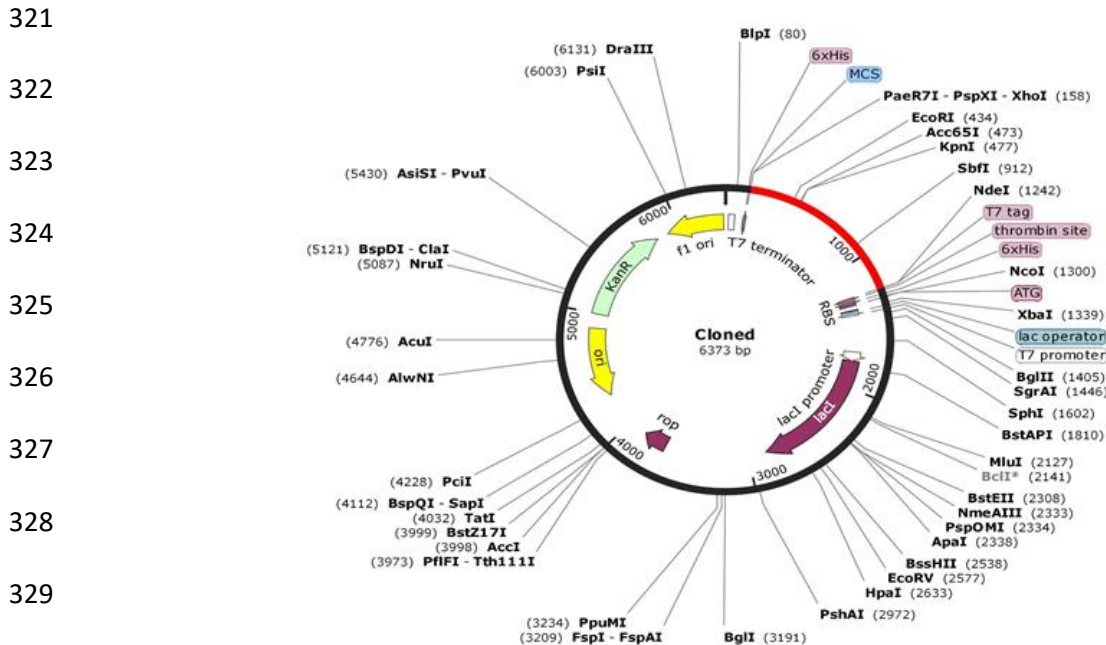
301



310 **Figure 7:** Molecular dynamics simulation of the receptor-vaccine complex. The left graph is
 311 showing the RMSD of the complex (X-axis = Time in ns and Y-axis = RMSD) while the right
 312 graph is showing the RMSF of the complex (X-axis = Time in residue and Y-axis = RMSF).
 313

314 Codon optimization and in silico cloning

315 To assure the maximal expression of the protein, vaccine codon was optimized in *E. coli* (strain
 316 k12) using Java Codon Adoption Tool. The optimized length of the codon sequence is 1077
 317 nucleotides. The average GC content was found 56.7% (optimum range 30%-70%) and CAI
 318 (codon adaption index) was 0.968, which indicates possibilities of good expression in host *E.*
 319 *coli*. Finally, using restriction enzymes restriction clone was formed and adapted codon sequence
 320 was inserted in pET28a (+) plasmid. The designed construct is shown in **Figure 8**.
 321



330

331 **Figure 8:** In silico restriction cloning of the final vaccine construct into pET28a (+) expression
332 vector where Red part representing the vaccine insert and black circle showing the vector.

333

334 **Discussion**

335 Norovirus proteins such as capsid, polyprotein, and protease were found antigenic and are vital
336 for infection and replication within the host. Therefore, they are considered very important for
337 subunit vaccine analysis. Immunization or vaccination is universally recognized method to
338 eradicate or control the infection. The advancement in computational approaches and their
339 applications to biological research ushered a new era of subunit vaccination designing in which
340 the most accurate or exact antigenic part is identified and used as an immunization tool instead of
341 the whole pathogen. The fast accumulation of vast genomic and proteomic data of pathogens
342 including norovirus is helpful in the development of epitope-based effective vaccines to control
343 and eradicate the diseases caused by various pathogens. Computational approaches predicted
344 epitopes (CTL & HTL) based on norovirus proteins and validation scores of these epitopes
345 suggest their use for subunit vaccine construction. MHC (major histocompatibility complex) is
346 of different types, MHC-I carry a peptide of 9-mer to the surface of the cell and act like an
347 impulsive signal for cytotoxic T cell. Which lead to cell destruction by activating immune
348 complementary cascade. MHC-II molecules present peptide of 15-mer to Helper T lymphocytes.
349 Our final subunit vaccine is composed of high-affinity CTL and HTL epitopes to elicit
350 immunity. The allergenicity and antigenicity values of the vaccine were calculated, and these
351 values indicate the non-allergen nature of the vaccine and are capable to provoke immune
352 response due to antigenic nature.

353 In addition to these epitopes, B cell linear epitopes were also predicted which help in B-cell
354 maturation, in order to produce antibodies. Physiochemical properties of vaccines such as
355 molecular weight, theoretical PI, aliphatic array and thermal stability were calculated. The
356 molecular weight of the vaccine was 36.560kDa, which is a suitable range for subunit vaccine;
357 the theoretical PI score is 9.17, which indicates that vaccine is basic in nature. The aliphatic array
358 suggests that vaccines have aliphatic side chains and instability index endorses the thermally
359 stable nature of the vaccine. For prediction and analysis of the secondary structure of vaccine,
360 PSIPRED V3.3 was used, which indicates the presence of 20.89% alpha-helix, 16.71% beta-
361 strand, and 62.39 % coil. Besides, the 3D structure obtained by homology modeling work
362 comprises of adequate information on the spatial arrangement of such essential protein residues
363 as well as useful guidance in the study of protein normal function, dynamics, and interaction
364 with ligand as well as other proteins. To pinpoint the error in the final 3D structure of vaccine
365 different structural validation tools were used to detect errors. From the main Ramachandran
366 plot, it was found that the overall model is satisfactory because most residues were found in the
367 most-favour region while few were present in the disordered region.

368 Furthermore, the vaccine was docked with TLR-7 in order to understand the immune response
369 towards vaccine final structure. Energy minimization was conducted to minimize the potential
370 energy of the entire system for the overall conformational stability of the docked vaccine protein-

371 TLR-7. Energy minimization repairs the structure's unnecessary topology by ditching certain
372 protein atoms and thus forms a more relatively stable structure with adequate stereochemistry is
373 thus formed.

374 To obtain maximum expression (transcription and translation) of vaccine protein in the host (*E.*
375 *coli* strain k-12), codon optimization was accomplished by CAI (codon adaptation index). The
376 solubility of overexpressed recombinant protein in the host (*E. coli*) is one of the crucial
377 requirements of many biochemical processes. Our vaccine protein shows a suitable proportion of
378 solubility in the host. The essential goals of many mechanical and biomedical applications are to
379 strengthen the protein. The newly designed vaccine was very effective and showing good
380 immunogenic response in animals, however, when these vaccines were applied to humans the
381 response was not similar due to the complexity of human immunopathology. In this study,
382 modern immunoinformatics approaches were incorporated to develop new thermostable, cheap
383 and effective subunit vaccines. These vaccines are safe and immunogenic to exploit the immune
384 system to provide protection from norovirus infection.

385 **Conclusion**

386 In this study, the main focus was to apply, *in-silico* approaches to design an effective multi-
387 epitope vaccine against norovirus based on three proteins due to their antigenic nature. To design
388 a vaccine, B and T cell epitopes were predicted, which is due to the presentation of pathogen
389 epitope by MHC-I and II. Suitable linkers were used to fuse these epitopes. Vaccine tertiary
390 structure was predicted and validated to ensure the functionality of the vaccine. The
391 physicochemical properties such as antigenicity, allergenicity, and stability were computed. The
392 vaccine was docked with TLR-7 to check the vaccine affinity towards the receptor.

393 Finally, for codon optimization, the protein was reversely translated which ensure maximum
394 expression of the vaccine in the host (*E. coli*). A wet lab experimental validation is needed to
395 assure the activity of constructed vaccine. This study can help in controlling norovirus infection.

396

397 **Methodology**

398 **Collection of *Norovirus* proteins for vaccine preparation**

399 The three proteins capsid, polyproteins, and small basic proteins were collected from UniProtKB
400 (<https://www.uniprot.org>) (33). These proteins were found antigenic through VaxiJen server
401 (<http://www.ddg-pharmfac.net/vaxijen/VaxiJen/VaxiJen.html>) and they were considered for
402 vaccine designing (34-36).

403

404 **Prediction of the (CTL) epitope**

405 NetCTL 1.2 is an online server (<http://www.cbs.dtu.dk/services/NetCTL/>) in which CTL
406 epitopes were predicted against these proteins (37). Prediction of these CTL epitopes is based
407 upon three essential parameters, including peptide attached to MHC-proteasomal C-terminal
408 degradation activity, TAP (Transporter Associated with Antigen Processing) delivery accuracy
409 and I. Artificial neural network was used to predict the attachment of peptide to MHC-I and

410 proteasomal C-terminal degradation while TAP deliverance score was predicted by the weight
411 matrix. For CTL epitope identification threshold was set as 0.75.

412

413 **Prediction of helper T-cell epitopes**

414 IEDB (Immune Epitope Database) is an online server (<http://tools.iedb.org/mhcii/>), which is
415 employed for prediction of Helper T cells lymphocytes of 15-mer length for five human alleles
416 (HLA-DRB1*01:01, HLA-DRB1*01:02, HLA-DRB1*01:03, HLA-DRB1*01:04, HLA-
417 DRB1*01:05) (38-40). This server speculates epitopes based on receptor affinity, which is
418 figured out from IC50 value (binding score) given to each epitope. Epitopes with higher binding
419 affinity mostly have IC50 score <50 nM. The IC50 value determines epitopes affinity, value such
420 is <500 nM represent moderate affinity while <5000 nM instantly show epitopes having low
421 affinity. The affinity of epitopes is inversely related to the value of percentile rank.

422

423 **Prediction of B cell lymphocytes**

424 ABCpred is an online server (<http://crdd.osdd.net/raghava/abcpred/>) employed for the prediction
425 of linear B-cell epitopes. The ABCpred predicts B-cell epitopes (linear) with a precision of 75%
426 (0.49 Sensitivity and 0.75 specificity). Conformational B-cell epitopes prediction is carried out
427 by DiscoTope 2.0 an online server (<http://www.cbs.dtu.dk/services/DiscoTope/>) (41). The
428 process of computation in this method is based on log-odds ratios (ratio among amino acid
429 composition in epitopes and residues of non-epitopes) and surface accessibility. The sensitivity
430 and specificity are found 0.47 and 0.75, respectively, on the default threshold (3.7).

431

432 **Multi-epitopes vaccine sequence construction**

433 High scoring epitopes including other parameters filtered out the final epitopes from CTL and
434 HTL. These selected epitopes were used to construct the final multi-epitopes subunit vaccine.
435 Linker such as AAY and GPGPG interconnect these epitope sand also enhanced effective
436 separation and presentation of epitopes. These linkers have two important roles; first, they assist
437 binding of HLA-II epitopes and also immune processing, and second, they restrain epitopes
438 numbers by specifying cleavage point (42-45). Further, to boost the immune responses an
439 adjuvant (TLR-7 agonist Beta-defensin 3 (Q5U7J2)) was affixed to the vaccine construct N-
440 terminus by EAAAK linker (46).

441 **Subunit vaccine and interferon**

442 Online server IFNepitope (<http://crdd.osdd.net/raghava/ifnepitope/predict.php>) assist in
443 designing and predicting the amino acid sequence from proteins, which have the potential to
444 release IFN-gamma from CD4+ T cells. This server helps in the designing of effective and better
445 subunit vaccine by identifying peptide which binds to MHC II and releases IFN-gamma (47)

446 **Prediction of vaccine allergenicity**

447 For allergenicity prediction of multi-epitope subunit vaccine AlgPred
448 (<http://crdd.osdd.net/raghava/algpred/>) web tool was used, in which algorithm like
449 (IgEpitope+SVMc+MAST+ARPs BLAST) was applied (48). This hybrid prediction veracity is

450 about 85% at 0.4 thresholds. The server employed six distant routes to act. These approaches
451 abet allergic protein prediction with perfection.

452

453 **Vaccine antigenicity prediction**

454 Online server ANTIGENpro (<http://scratch.proteomics.ics.uci.edu/>) was used for antigenicity
455 prediction (49). Server to predict protein antigenicity used two approaches; primary protein
456 sequence is presented multiple time, and five different machine-learning algorithms were applied
457 to produce the result based on protein microarray data analysis.

458

459 **Physiochemical parameters and identification of domain**

460 ProtParam (<http://web.expasy.org/protparam/>), an online server was used for the prediction of
461 many physiochemical parameters such as theoretical PI, instability index, amino acid
462 composition, in vitro and in vivo half-life, molecular weight, aliphatic index and also the
463 (GRAVY) which is a grand average of hydropathicity (50).

464

465 **Prediction of secondary structure**

466 The primary amino-acid sequence was used to predict the secondary structure of Protein by
467 PDBsum. Sequences that shows homology to vaccine protein were selected for structure
468 prediction. Position position-specific iterated (PSI-BLAST) identified homologous residues.

469

470 **Prediction of the tertiary structure**

471 For prediction and analysis of protein tertiary structure, an online server Robetta
472 (<http://rosetta.bakerlab.org>) was utilized, which is an automated tool(51). Protein sequences were
473 submitted in FASTA format to predict 3D structure. Models were generated after parsing the
474 structure into respective domains. This model is based either on comparative modelling or de
475 novo structure; for comparative modelling homologs sequence was identified by BLAST, 3D-
476 Jury or FFAS03, and PSI-BLAST, which is then used as a templet. If homologs were not found,
477 de novo structure was generated using Rosetta fragment insertion method.

478

479 **Validation of tertiary structure**

480 To validate the predicted model is an essential step, ProSA-web an online server
481 (<https://prosa.services.came.sbg.ac.at/prosa.php>) was used for validation of tertiary structure. For
482 input structure, overall quality scoring was computed. The predicted protein will have an error
483 when the scoring characteristic was found arbitrary then native proteins. For statistical analysis
484 of non-bonded interaction ERRAT server was used (<https://servicesn.mbi.ucla.edu/ERRAT/>)
485 (52), and Ramachandran plot analysis was performed on RAMPAGE server
486 (<http://mordred.bioc.cam.ac.uk/~rapper/rampage.php>) (53). This server utilized PROCHECK
487 principle to validate the structure of protein through Ramachandran plot and separate plots for
488 Proline and Glycine residues.

489

490 **Vaccine and TLR-7 Docking**

491 ZDOCK server (<http://zdock.umassmed.edu/>) was used for the docking of the final vaccine with
492 TLR-7 (54). The ZDOCK webserver produces quick and accurate complexes. Refinement and
493 post-processing of the complexes were subjected to Firedock server(55).

494

495 **MD (Molecular dynamic simulation) of Receptor-Vaccine complex**

496 For selected complexes, amber 14 (56) was used to conduct MD simulation. The system was
497 neutralized and solvated with TIP3P water box. Two stages of energy minimization, followed by
498 gentle heating and equilibration, were performed (57). After equilibration, 30ns simulation was
499 conducted. For post-simulation trajectories analysis (RMSD and RMSF), 2.0 ps time scale was
500 used and for trajectory, sampling using CPPTRAJ and PTRAJ(58)implemented in AMBER 14.

501

502 **Codon optimization and in silico cloning of vaccine**

503 For effective expression of the vaccine in a host (*E. coli* strain K12) was performed. Reverse
504 translation and codon optimization were performed using JCAT (Java Codon Adaption tool).
505 Norovirus genome expression is distinct from the expression of vector genome, codon
506 optimization ensures maximum expression of vaccine with in the vector. In order to get the
507 desired result, three additional options were selected, such as prokaryote ribosome binding site,
508 restriction enzymes cleavage and rho-independent transcription termination. JCat output includes
509 a codon adaptation index (CAI) and to ensure the high-level protein expression percentage GC
510 content is used (25). In order to clone the desired gene in *E. coli* pET-28a (+) two restriction sites
511 NdeI and XhoI were added to the C and N terminal of the sequence, respectively. Finally, the
512 adapted sequence having the restriction site was inserted to pET-28a (+) to maximize the vaccine
513 expression.

514

515 **Acknowledgements:**

516 Dong-Qing Wei is supported by the grants from the Key Research Area Grant 2016YFA0501703
517 of the Ministry of Science and Technology of China, the National Natural Science Foundation of
518 China (Contract no. 61832019, 61503244), the Science and Technology Commission of
519 Shanghai Municipality (Grant: 19430750600), the Natural Science Foundation of Henan
520 Province (162300410060) and Joint Research Funds for Medical and Engineering and Scientific
521 Research at Shanghai Jiao Tong University (YG2017ZD14). The computations were partially
522 performed at the Pengcheng Lab and the Center for High-Performance Computing, Shanghai
523 Jiao Tong University.

524

525

526

527

528

530 **ReferencesPrimary Sources**

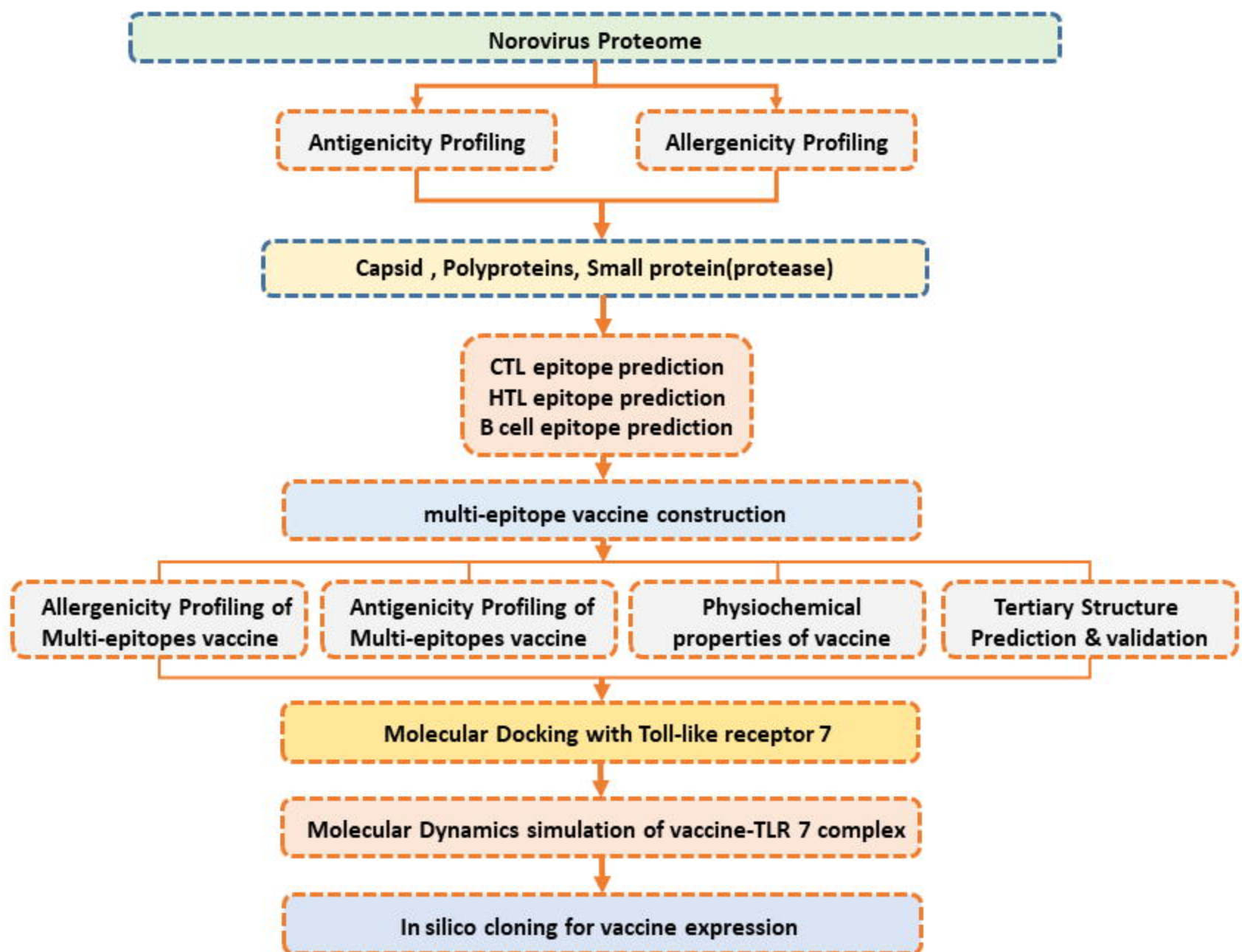
531 **Secondary Sources**

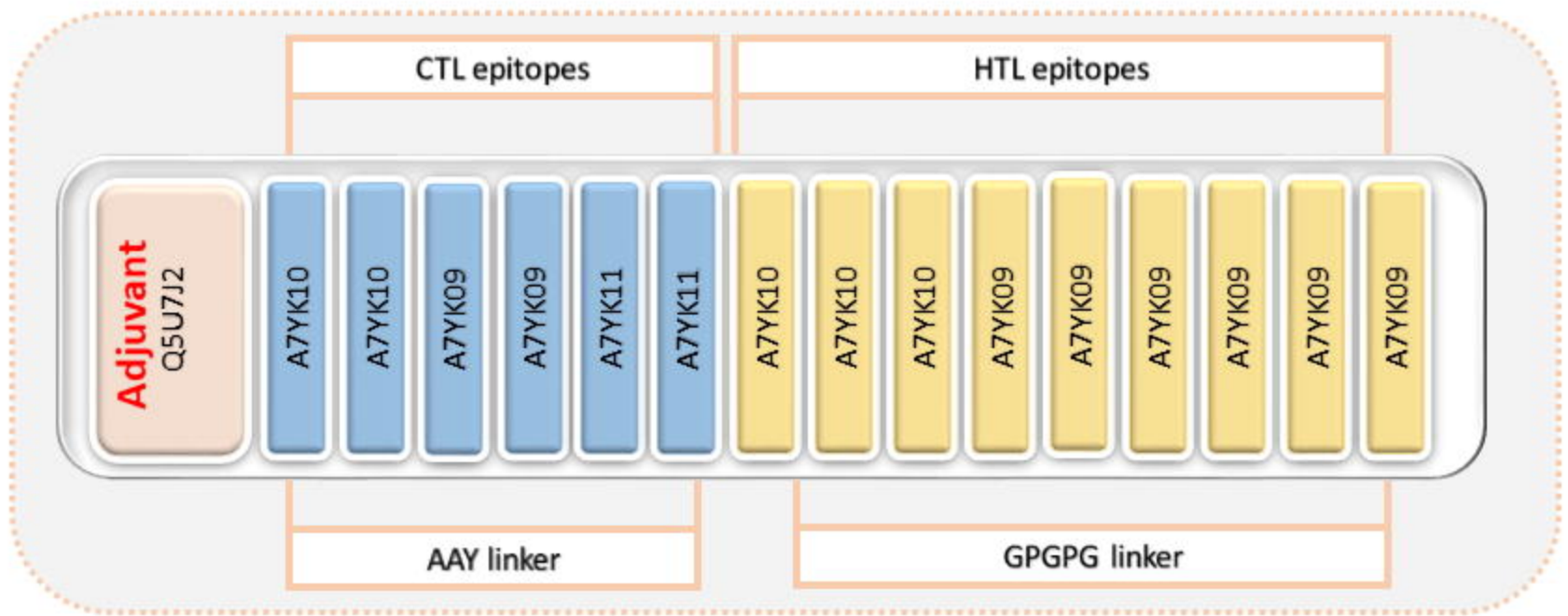
532 **Uncategorized References**

- 533 1. Lew, J. F., Kapikian, A. Z., Valdesuso, J. and Green, K. Y. (1994) title. *The Journal of infectious diseases*
534 170, 535-542.
- 535 2. Robilotti, E., Deresinski, S. and Pinsky, B. A. (2015) title. *Clinical microbiology reviews* 28, 134-164.
- 536 3. White, M. B., Rajagopalan, S. and Yoshikawa, T. T. (2016) title. *Clinics in geriatric medicine* 32, 509-
537 522.
- 538 4. Mead, P. S., Slutsker, L., Dietz, V., McCaig, L. F., Bresee, J. S., Shapiro, C., Griffin, P. M. and Tauxe, R. V.
539 (1999) title. *Emerging infectious diseases* 5, 607-625.
- 540 5. Ahmed, S. M., Hall, A. J., Robinson, A. E., Verhoef, L., Premkumar, P., Parashar, U. D., Koopmans, M.
541 and Lopman, B. A. (2014) title. *The Lancet. Infectious diseases* 14, 725-730.
- 542 6. Pires, S. M., Fischer-Walker, C. L., Lanata, C. F., Devleesschauwer, B., Hall, A. J., Kirk, M. D., Duarte, A.
543 S., Black, R. E. and Angulo, F. J. (2015) title. *PloS one* 10, e0142927.
- 544 7. Mattison, C. P., Cardemil, C. V. and Hall, A. J. (2018) title. *Expert review of vaccines* 17, 773-784.
- 545 8. McFadden, N., Bailey, D., Carrara, G., Benson, A., Chaudhry, Y., Shortland, A., Heeney, J., Yarovinsky,
546 F., Simmonds, P., Macdonald, A. and Goodfellow, I. (2011) title. *PLoS pathogens* 7, e1002413.
- 547 9. Caul, E. and Appleton, H. (1982) title. *Journal of medical virology* 9, 257-265.
- 548 10. Ando, T., Monroe, S. S., Gentsch, J. R., Jin, Q., Lewis, D. C. and Glass, R. I. (1995) title. *Journal of*
549 *Clinical Microbiology* 33, 64-71.
- 550 11. Green, J., Norcott, J., Lewis, D., Arnold, C. and Brown, D. (1993) title. *Journal of Clinical Microbiology*
551 31, 3007-3012.
- 552 12. Norcott, J., Green, J., Lewis, D., Estes, M., Barlow, K. and Brown, D. (1994) title. *Journal of medical*
553 *virology* 44, 280-286.
- 554 13. Vinje, J. and Koopmans, M. P. (1996) title. *Journal of Infectious Diseases* 174, 610-615.
- 555 14. Fankhauser, R. L., Noel, J. S., Monroe, S. S., Ando, T. and Glass, R. I. (1998) title. *The Journal of*
556 *infectious diseases* 178, 1571-1578.
- 557 15. Maguire, A. J., Green, J., Brown, D. W., Desselberger, U. and Gray, J. J. (1999) title. *Journal of Clinical*
558 *Microbiology* 37, 81-89.
- 559 16. Mattick, K. L., Green, J., Punia, P., Belda, F. J., Gallimore, C. I. and Brown, D. W. (2000) title. *Journal of*
560 *virological methods* 87, 161-169.
- 561 17. Kreis, S. and Whistler, T. (1997) title. *Virus research* 47, 197-203.
- 562 18. Chezzi, C. and Schoub, B. D. (1996) title. *Journal of virological methods* 62, 93-102.
- 563 19. Weiner, A., Houghton, M., Polito, A., Massaro, A., Bonino, F., Brunetto, M., Danielle, F., Calabrese,
564 G., Guaschino, R. and Dinello, R. (1998) title.
- 565 20. Kapikian, A. Z., Wyatt, R. G., Dolin, R., Thornhill, T. S., Kalica, A. R. and Chanock, R. M. (1972) title.
566 *Journal of virology* 10, 1075-1081.
- 567 21. Cortes-Penfield, N. W., Trautner, B. W. and Jump, R. L. P. (2017) title. *Infect Dis Clin North Am* 31,
568 673-688.
- 569 22. Pulendran, B. and Ahmed, R. (2011) title. *Nature immunology* 12, 509-517.
- 570 23. Dash, R., Das, R., Junaid, M., Akash, M. F. C., Islam, A. and Hosen, S. Z. (2017) title. *Adv Appl*
571 *Bioinform Chem* 10, 11-28.
- 572 24. Adhikari, U. K., Tayebi, M. and Rahman, M. M. (2018) title. *Journal of Immunology Research* 2018,
573 22.

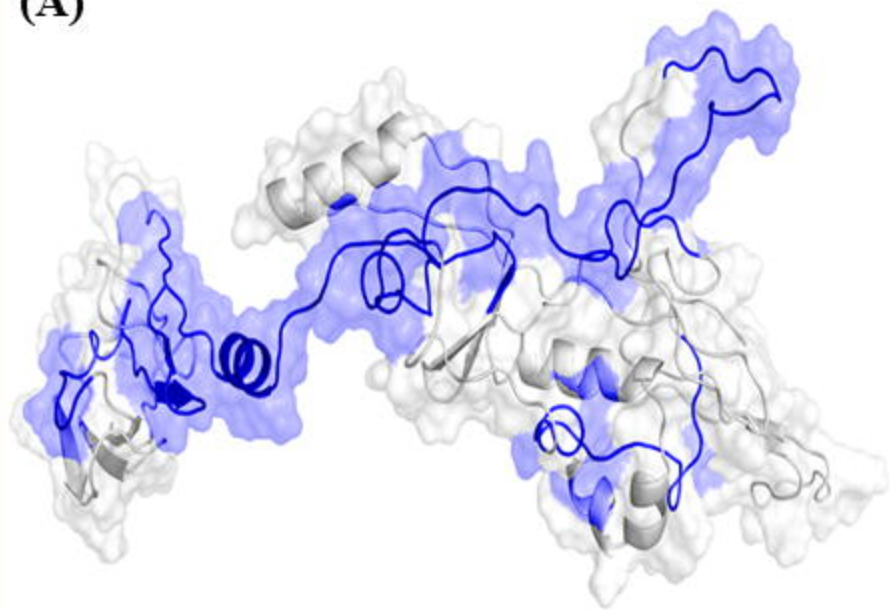
- 574 25. Khan, S., Khan, A., Rehman, A. U., Ahmad, I., Ullah, S., Khan, A. A., Ali, S. S., Afridi, S. G. and Wei, D.
575 Q. (2019) title. *Infection, genetics and evolution : journal of molecular epidemiology and evolutionary*
576 *genetics in infectious diseases* 73, 390-400.
- 577 26. Kaliamurthi, S., Selvaraj, G., Junaid, M., Khan, A., Gu, K. and Wei, D.-Q. (2018) title. *Current*
578 *pharmaceutical design* 24, 3791-3817.
- 579 27. Khan, A., Junaid, M., Kaushik, A. C., Ali, A., Ali, S. S., Mehmood, A. and Wei, D.-Q. (2018) title. *PLoS*
580 *one* 13.
- 581 28. Rappuoli, R. (2000) title. *Current Opinion in Microbiology* 3, 445-450.
- 582 29. Sette, A. and Fikes, J. (2003) title. *Current opinion in immunology* 15, 461-470.
- 583 30. Agrawal, P. and Raghava, G. P. S. (2018) title. *Frontiers in microbiology* 9, 2551.
- 584 31. Khan, M., Khan, S., Ali, A., Akbar, H., Sayaf, A. M., Khan, A. and Wei, D.-Q. (2019) title. *Scientific*
585 *reports* 9, 1-13.
- 586 32. Ali, A., Khan, A., Kaushik, A. C., Wang, Y., Ali, S. S., Junaid, M., Saleem, S., Cho, W. C., Mao, X. and
587 Wei, D.-Q. (2019) title. *Scientific reports* 9, 1-12.
- 588 33. Consortium, T. U. (2018) title. *Nucleic Acids Research* 47, D506-D515.
- 589 34. Doytchinova, I. A. and Flower, D. R. (2007) title. *BMC bioinformatics* 8, 4.
- 590 35. Doytchinova, I. A. and Flower, D. R. (2007) title. *Vaccine* 25, 856-866.
- 591 36. Doytchinova, I. A. and Flower, D. R. (2008) title. *Open Vaccine J* 1, 4.
- 592 37. Larsen, M. V., Lundegaard, C., Lamberth, K., Buus, S., Lund, O. and Nielsen, M. (2007) title. *BMC*
593 *Bioinformatics* 8, 424.
- 594 38. Wang, P., Sidney, J., Kim, Y., Sette, A., Lund, O., Nielsen, M. and Peters, B. (2010) title. *BMC*
595 *Bioinformatics* 11, 568.
- 596 39. Wang, P., Sidney, J., Dow, C., Mothe, B., Sette, A. and Peters, B. (2008) title. *PLoS computational*
597 *biology* 4, e1000048.
- 598 40. Nielsen, M. and Lund, O. (2009) title. *BMC Bioinformatics* 10, 296.
- 599 41. Kringelum, J. V., Lundegaard, C., Lund, O. and Nielsen, M. (2012) title. *PLoS computational biology* 8,
600 e1002829.
- 601 42. Saadi, M., Karkhah, A. and Nouri, H. R. (2017) title. *Infection, Genetics and Evolution* 51, 227-234.
- 602 43. Livingston, B., Crimi, C., Newman, M., Higashimoto, Y., Appella, E., Sidney, J. and Sette, A. (2002)
603 title. *The Journal of Immunology* 168, 5499-5506.
- 604 44. Dorosti, H., Eslami, M., Negahdaripour, M., Ghoshoon, M. B., Gholami, A., Heidari, R., Dehshahri, A.,
605 Erfani, N., Nezafat, N. and Ghasemi, Y. (2019) title. *Journal of Biomolecular Structure and Dynamics* 37,
606 3524-3535.
- 607 45. Bergmann, C. C., Yao, Q., Ho, C. K. and Buckwold, S. L. (1996) title. *The Journal of Immunology* 157,
608 3242-3249.
- 609 46. Arai, R., Ueda, H., Kitayama, A., Kamiya, N. and Nagamune, T. (2001) title. *Protein engineering* 14,
610 529-532.
- 611 47. Dhanda, S. K., Vir, P. and Raghava, G. P. S. (2013) title. *Biology Direct* 8, 30.
- 612 48. Saha, S. and Raghava, G. P. S. (2006) title. *Nucleic Acids Research* 34, W202-W209.
- 613 49. Cheng, J., Randall, A. Z., Sweredoski, M. J. and Baldi, P. (2005) title. *Nucleic Acids Research* 33, W72-
614 W76.
- 615 50. Gasteiger, E., Hoogland, C., Gattiker, A., Duvaud, S. e., Wilkins, M. R., Appel, R. D. and Bairoch, A.
616 (2005) *Protein Identification and Analysis Tools on the ExPASy Server*, in *The Proteomics Protocols*
617 *Handbook*, (J. M. Walker ed, Humana Press, Totowa, NJ: pp. 571-607.
- 618 51. Kim, D. E., Chivian, D. and Baker, D. (2004) title. *Nucleic acids research* 32, W526-W531.
- 619 52. Colovos, C. and Yeates, T. O. (1993) title. *Protein science* 2, 1511-1519.
- 620 53. Colovos, C. and Yeates, T. O. (1993) title. *Protein science : a publication of the Protein Society* 2,
621 1511-1519.

- 622 54. Enosi Tuipulotu, D., Netzler, N. E., Lun, J. H., Mackenzie, J. M. and White, P. A. (2018) title. 62.
623 55. Pierce, B. G., Wiehe, K., Hwang, H., Kim, B.-H., Vreven, T. and Weng, Z. (2014) title. *Bioinformatics*
624 30, 1771-1773.
625 56. Pearlman, D. A., Case, D. A., Caldwell, J. W., Ross, W. S., Cheatham, T. E., DeBolt, S., Ferguson, D.,
626 Seibel, G. and Kollman, P. (1995) title. *Computer Physics Communications* 91, 1-41.
627 57. Salomon-Ferrer, R., Case, D. A. and Walker, R. C. (2013) title. *Wiley Interdisciplinary Reviews:*
628 *Computational Molecular Science* 3, 198-210.
629 58. Roe, D. R. and Cheatham, T. E. (2013) title. *Journal of Chemical Theory and Computation* 9, 3084-
630 3095.
- 631

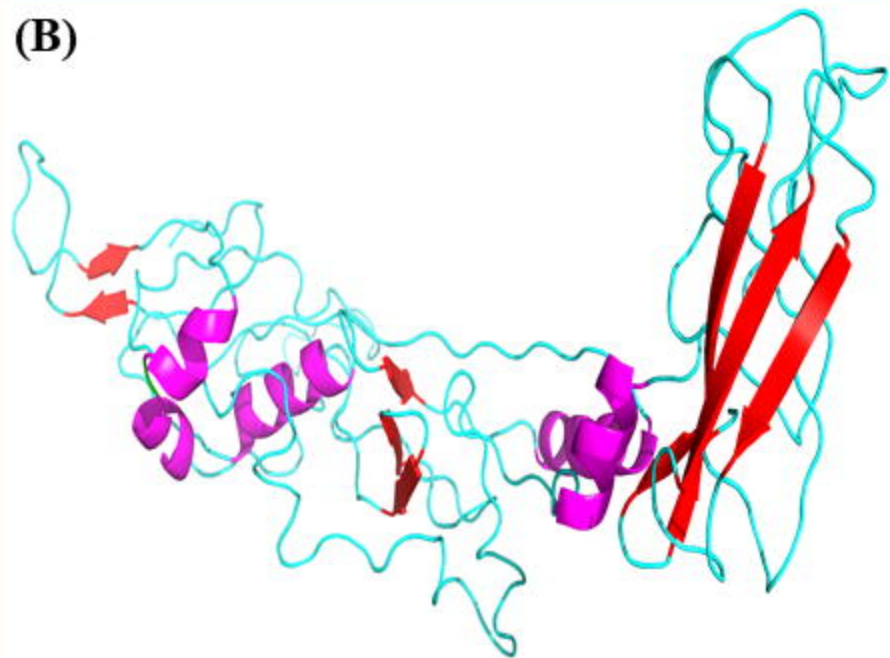


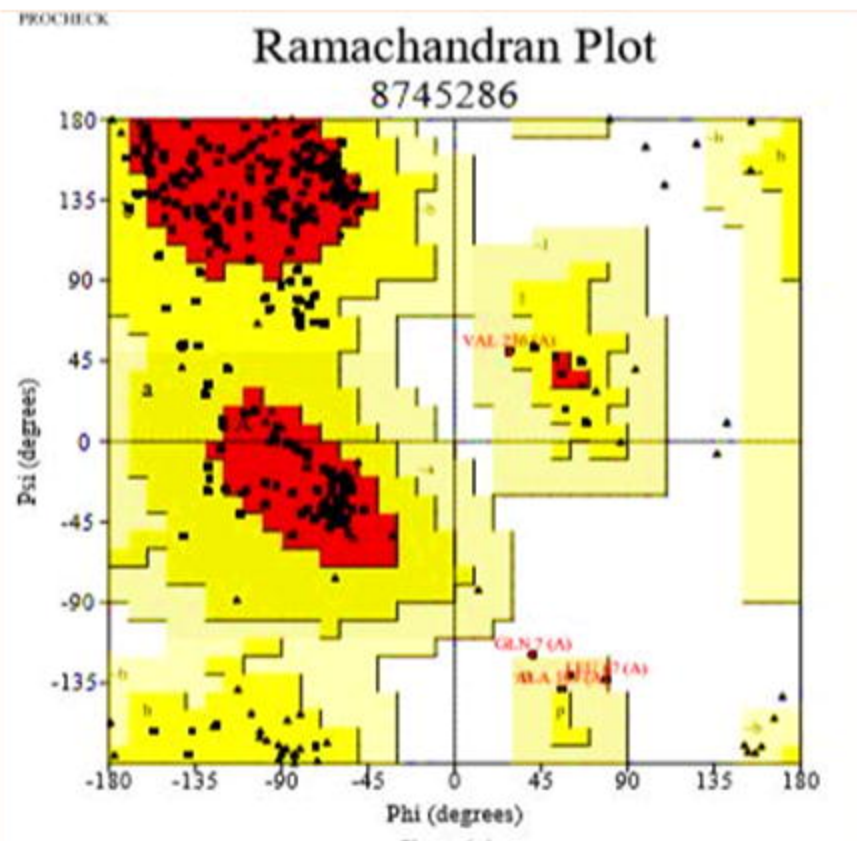
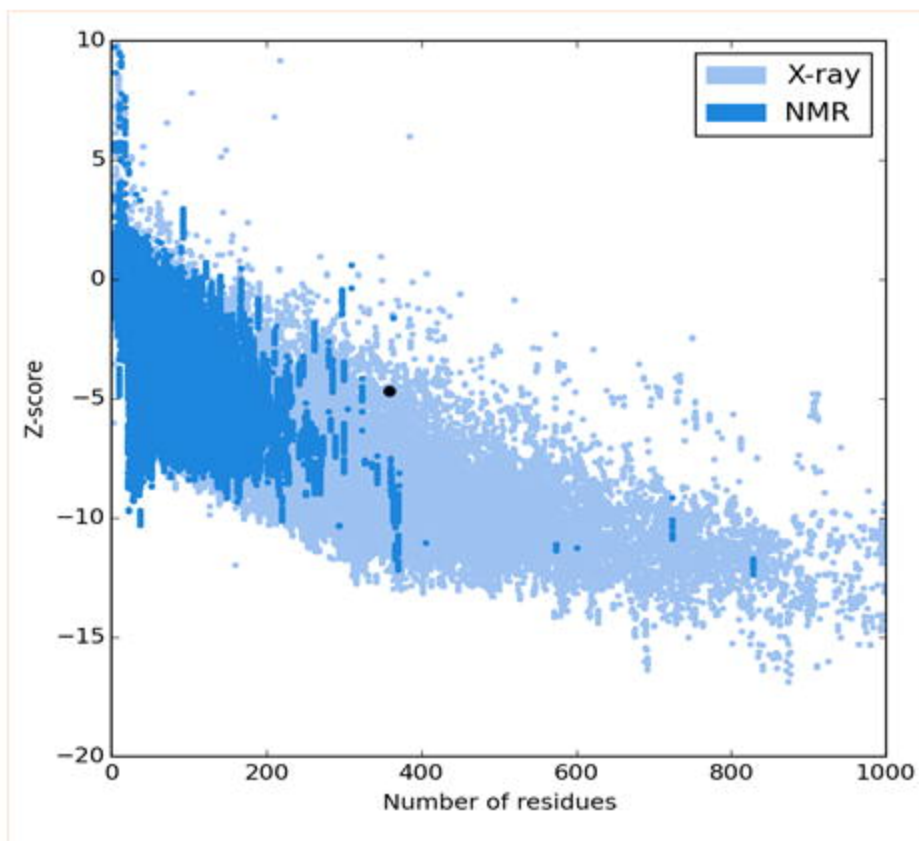


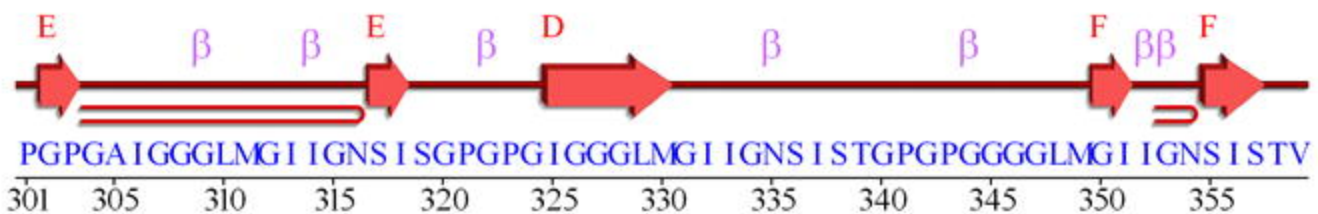
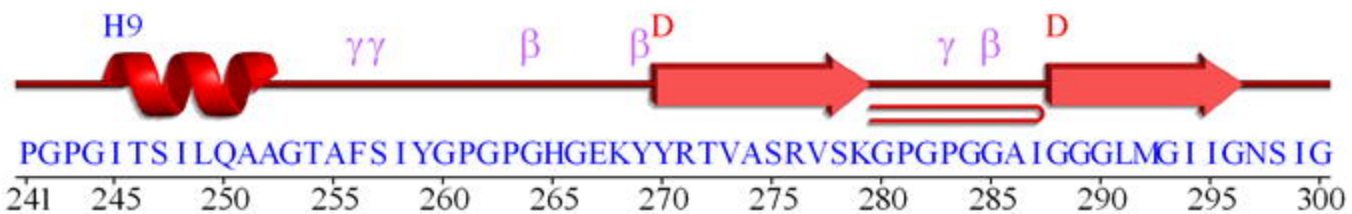
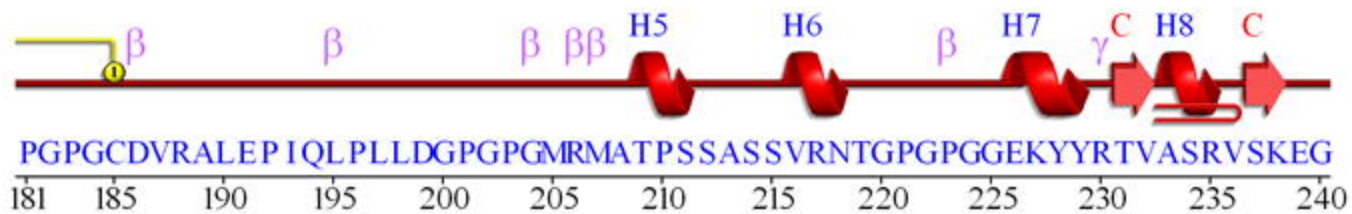
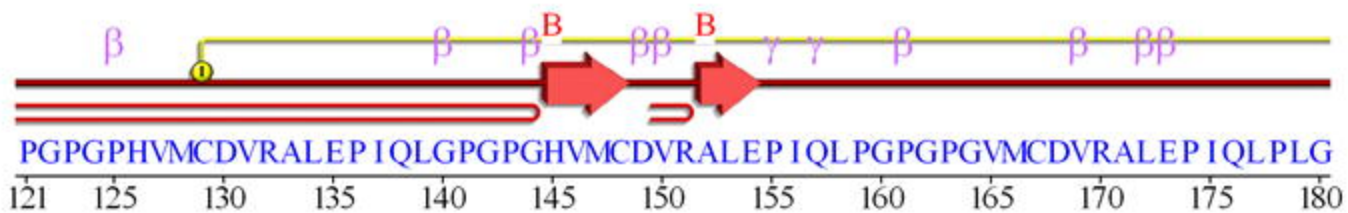
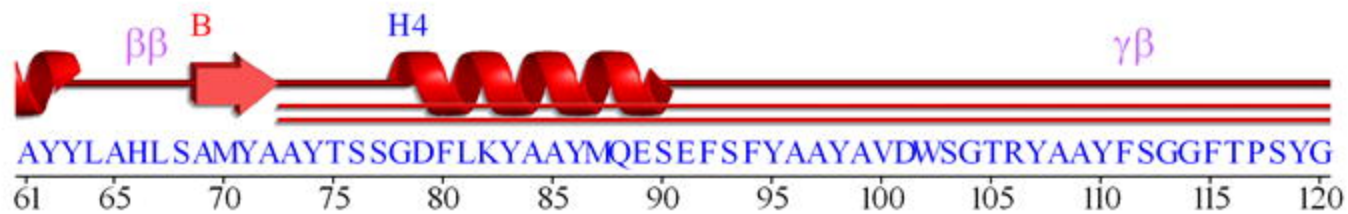
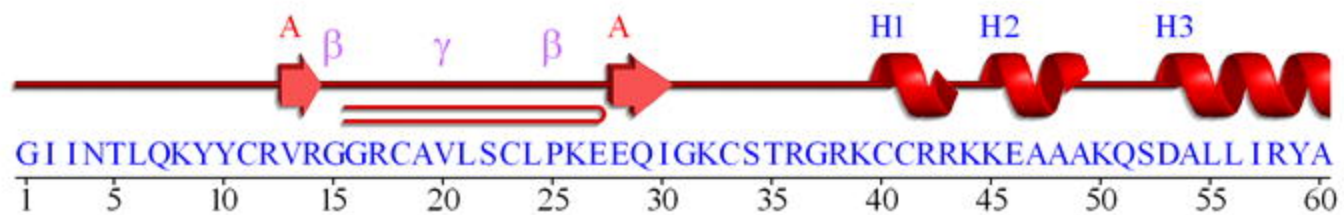
(A)



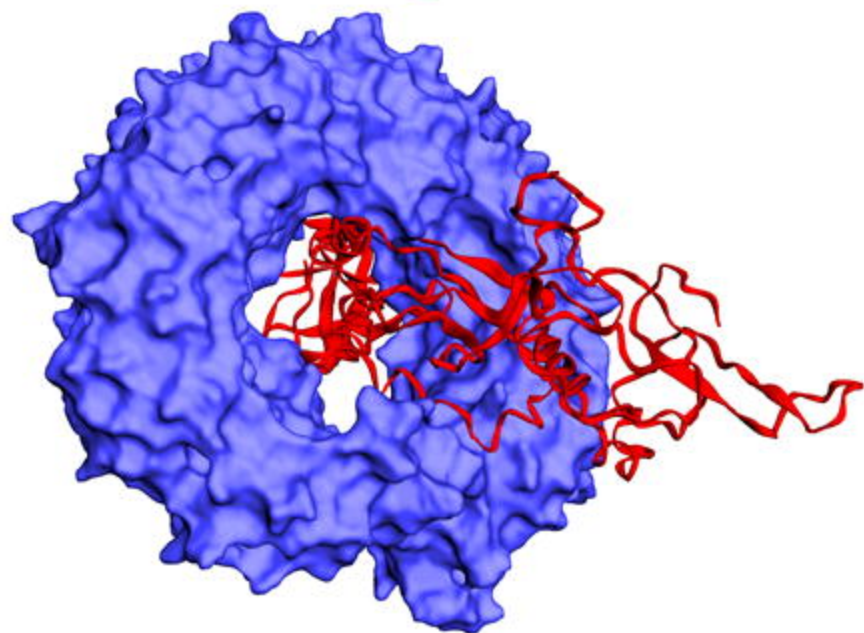
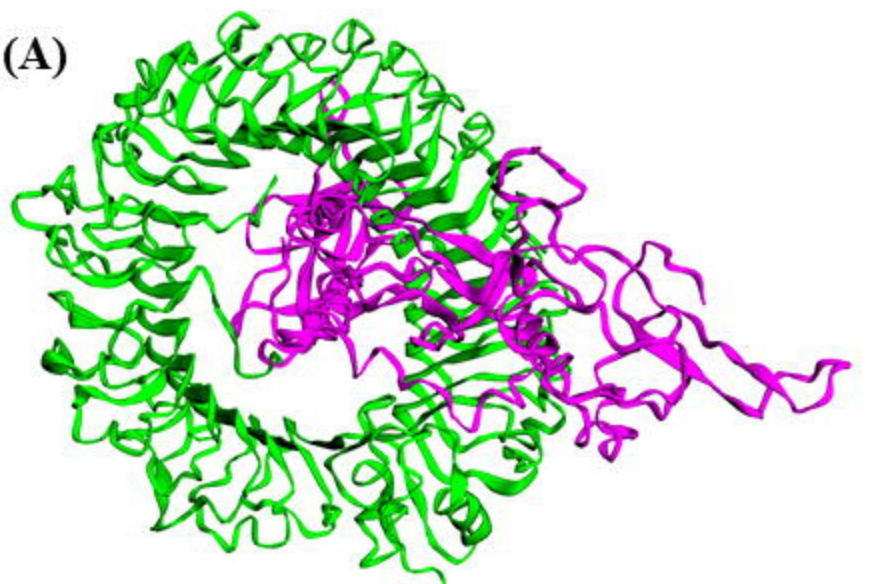
(B)



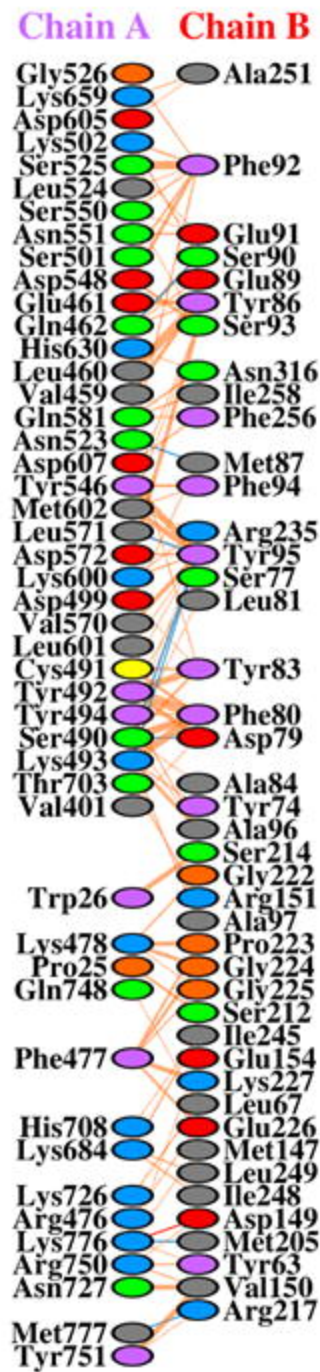




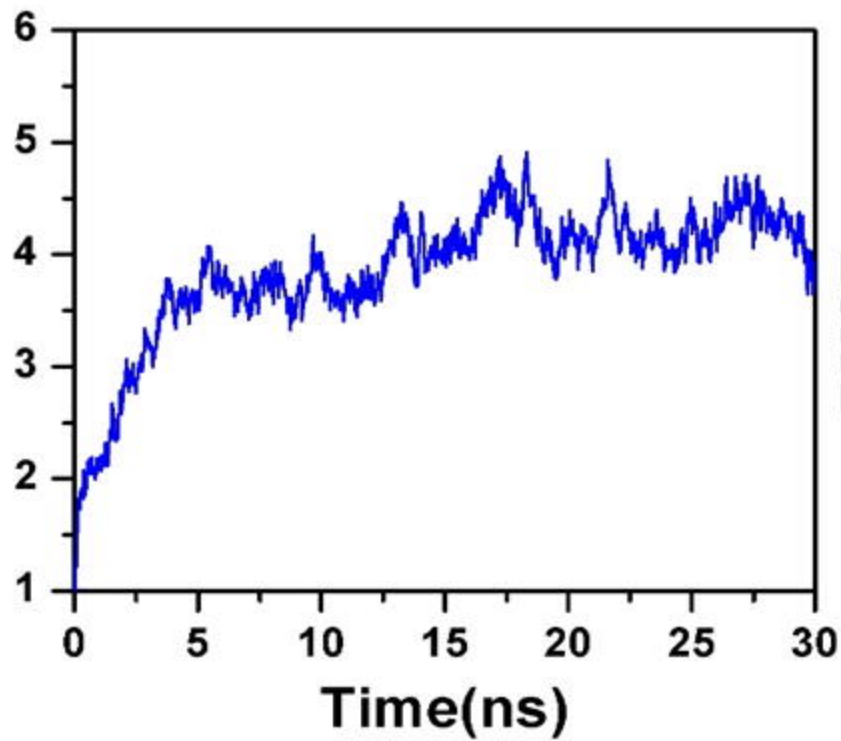
(A)



(B)



RMSD



RMSF

